Biomaterials 100 (2016) 53–66

Contents lists available at ScienceDirect

Biomaterials

journal homepage: www.elsevier.com/locate/biomaterials

Non-virally engineered human adipose mesenchymal stem cells produce BMP4, target brain tumors, and extend survival

Antonella Mangraviti [a, 2], Stephany Y. Tzeng [b, 2, 1], David Gullotti [a], Kristen L. Kozielski [b], Jennifer E. Kim [a], Michael Seng [a], Sara Abbadi [a, c], Paula Schiapparelli [a, c], Rachel Sarabia-Estrada [a, c], Angelo Vescovi [e], Henry Brem [a, b, c, d], Alessandro Olivi [a, c], Betty Tyler [a, c, **], Jordan J. Green [a, b, c, d, ***], Alfredo Quinones-Hinojosa [a, c, *]

[a] Department of Neurosurgery, Johns Hopkins University School of Medicine, Baltimore, MD, USA
[b] Department of Biomedical Engineering, Johns Hopkins School of Medicine, Baltimore, MD, USA
[c] Department of Oncology, Johns Hopkins University School of Medicine, Baltimore, MD, USA
[d] Department of Ophthalmology, Johns Hopkins University School of Medicine, Baltimore, MD, USA
[e] IRCSS Casa Sollievo della Sofferenza, Opera di San Pio da Pietrelcina, viale dei Cappuccini, 1, 71013 S. Giovanni Rotondo, Italy

ARTICLE INFO

Article history:
Received 30 March 2016
Received in revised form
16 May 2016
Accepted 18 May 2016
Available online 21 May 2016

Keywords:
Brain cancer
Adipose-derived stem cells
Nanoparticles
Gene delivery
Tumor stem cells

ABSTRACT

There is a need for enabling non-viral nanobiotechnology to allow safe and effective gene therapy and cell therapy, which can be utilized to treat devastating diseases such as brain cancer. Human adipose-derived mesenchymal stem cells (hAMSCs) display high anti-glioma tropism and represent a promising delivery vehicle for targeted brain tumor therapy. In this study, we demonstrate that non-viral, biodegradable polymeric nanoparticles (NPs) can be used to engineer hAMSCs with higher efficacy (75% of cells) than leading commercially available reagents and high cell viability. To accomplish this, we engineered a poly(beta-amino ester) (PBAE) polymer structure to transfect hAMSCs with significantly higher efficacy than Lipofectamine™ 2000. We then assessed the ability of NP-engineered hAMSCs to deliver bone morphogenetic protein 4 (BMP4), which has been shown to have a novel therapeutic effect by targeting human brain tumor initiating cells (BTIC), a source of cancer recurrence, in a human primary malignant glioma model. We demonstrated that hAMSCs genetically engineered with polymeric nanoparticles containing BMP4 plasmid DNA (BMP4/NP-hAMSCs) secrete BMP4 growth factor while maintaining their multipotency and preserving their migration and invasion capacities. We also showed that this approach can overcome a central challenge for brain therapeutics, overcoming the blood brain barrier, by demonstrating that NP-engineered hAMSCs can migrate to the brain and penetrate the brain tumor after both intranasal and systemic intravenous administration. Critically, athymic rats bearing human primary BTIC-derived tumors and treated intranasally with BMP4/NP-hAMSCs showed significantly improved survival compared to those treated with control GFP/NP-hAMCSs. This study demonstrates that synthetic polymeric nanoparticles are a safe and effective approach for stem cell-based cancer-targeting therapies.

1. Introduction

Over 20,000 new cases of malignant brain cancer are diagnosed in the United States every year, causing nearly 15,000 deaths each year [1,2]. The most common of malignant brain tumors are glioblastoma (GBM), a grade IV astrocytoma with an estimated 5% five-year survival rate. Even with the current gold standard of treatment, including surgery, chemotherapy, and radiotherapy, GBM patients have a median survival of approximately 15 months [3–5]. This dire prognosis, which has improved only incrementally in the

Abbreviations: NP, nanoparticle; hAMSC, human adipose-derived mesenchymal stem cell; PBAE, poly(beta-amino ester); BMP4, bone morphogenic protein.

* Corresponding author. Department of Neurosurgery, Johns Hopkins University School of Medicine, Baltimore, MD, USA.
** Corresponding author. Department of Neurosurgery, Johns Hopkins University School of Medicine, Baltimore, MD, USA.
*** Corresponding author. Biomedical Engineering, Johns Hopkins University School of Medicine, Baltimore, MD, USA.
E-mail addresses: btyler@jhmi.edu (B. Tyler), green@jhu.edu (J.J. Green), aquinon2@jhmi.edu (A. Quinones-Hinojosa).
[1] David H. Koch Institute for Integrative Cancer Research, Massachusetts Institute of Technology, Cambridge, MA.
[2] These authors contributed equally.

http://dx.doi.org/10.1016/j.biomaterials.2016.05.025
0142-9612/

last decades, prompts the development of novel treatment strategies. Among the challenges of GBM treatment is the difficulty of drug delivery to the tumor site without significant adverse side effects, particularly when using a systemic route of administration [6]. For efficacy, a therapeutic must reach the brain in sufficient concentration after crossing the blood-brain barrier (BBB) [7], be able to diffuse [8] or otherwise move through the brain parenchyma [9,10], and ideally have an effect on cancer cells instead of healthy cells, including malignant cells that invade the tissue surrounding the main tumor site [11].

One intriguing method of targeted delivery to brain tumors is the use of adult stem cells as vehicles that can carry a therapeutic payload [12,13], with mesenchymal stem cells (MSCs) among the most attractive candidates for cell-based therapy. MSCs can cross the BBB and have been shown to have innate tumor tropism, and their low immunogenicity also enables transplantations of both autologous and heterologous MSCs [14]. After being genetically engineered, they can secrete therapeutic agents directly into the tumor [15,16], and such engineered stem cells have already produced impressive results in preclinical glioma models [17]. MSCs have been successfully used as brain tumor-targeting carriers of prodrug/drug systems [18,19] or cytokines and proteins such as IFN-beta [20], tumor necrosis factor-related apoptosis-inducing ligand (TRAIL) alone or in combination with radiation or temozolomide [16,21,22], and bone morphogenic factor 4 (BMP4), a growth factor known to decrease the tumorigenicity of brain tumor initiating cells (BTICs) [23,24]. We have previously reported that human adipose-derived mesenchymal stem cells (hAMSCs) display brain tumor tropism, can be successfully used as brain tumor-targeting carriers, and have antiglioma effects *in vivo* when genetically engineered to deliver BMP4 to target BTICs [23,25–28]. The hAMSCs were also shown to be non-oncogenic, and they did not proliferate *in vivo*, instead decreasing in number after 2 weeks, reducing the chance of adverse effects due to the cells. Viral vectors have thus far been the most widely used method of engineering hAMSCs to carry tumor-targeting proteins and are well known to have high gene delivery efficiency. However they carry the risk of immunotoxicity related to viral proteins or replication, which can cause a decrease in the gene delivery efficiency because of containment by host antibodies [29]. Moreover, viral antigens may activate latent viruses and cause inflammatory responses [30] or facilitate autoimmunity, leading to demyelination [31] or neurodegeneration [32,33]. In addition, foreign promoters inserted into virus genomes rarely behave as they would in their natural genomic setting, and virus tropism is highly dependent on host cell permissiveness at the transcriptional level. Still, the wide use of these vectors in the human population has inspired general confidence on their relative safety [29]. However, the unsatisfactory results of the first large-scale phase III trial of gene therapy for brain tumors [34] have again raised questions about the level, tropism and consistency of virus titers in the brain [35], resurrecting safety concerns related to the use of virus at high titers and the need for a different option. In this era, when the application of nanotechnology is driving tremendous progress in medicine, research on a safer and equally effective non-viral option among nanoparticle vectors has become an appealing answer to this challenging question.

Moreover, an alternative strategy to viral transduction, such as non-viral transfection by synthetic nanoparticles (NPs), could lead to the safe application of MSC-based therapies across a broad spectrum of diseases and indications. Non-viral vectors carry low risk of insertional mutagenesis, are not restricted by plasmid size, and can be produced more quickly and easily than viral vectors. However, common non-viral materials used for gene transfer, including lipids such as commercially available Lipofectamine™ 2000 and synthetic polymers such as polyethylenimine are often limited by cytotoxicity and low efficacy [36–39]. In this study, we used poly(beta-amino ester)s (PBAEs), biodegradable cationic polymers with significant potential for non-viral gene delivery. Easily synthesized and rapidly screened [40,41], PBAEs self-assemble into NPs with nucleic acids via electrostatic interactions, enabling effective gene delivery of different types of human cell lines with high efficacy and low cytotoxicity [42,43].

We used reporter genes to demonstrate very high non-viral transfection of hAMSCs with PBAE NPs (75 ± 2% positive cells by flow cytometry). Next, we genetically engineered hAMSCs to produce BMP4 in order to target BTICs in malignant gliomas. We also evaluated the effect of non-viral transfection, as compared to viral transduction, on the migration, invasion, and multipotency of hAMSCs and found that our synthetic gene delivery devices had a relatively benign effect on cells. In addition, we provide *in vivo* evidence that NP-engineered hAMSCs administered locally and systemically in a rodent glioma model retain their intrinsic tumor-homing efficiency by migrating towards the brain and penetrating the tumor, and hAMSCs engineered to secrete BMP4 significantly increased survival in BTIC-bearing rats. To our knowledge, this is the first study showing that *in vivo* administration of hAMSCs genetically engineered with PBAE nanoparticles has a significant therapeutic effect in a human malignant glioma model. These biodegradable synthetic nanoparticles are a safe and efficient alternative to viral transduction and engineering of human stem cells that can be applied to a wide array of diseases.

2. Materials and methods

2.1. Experimental design

Poly(beta-amino ester)s (PBAEs) were complexed with DNA plasmids and used to transfect human adipose mesenchymal stem cells (hAMSCs) to identify the optimal formulations for transfection efficacy and cell viability (Scheme 1A). *In vitro* assays were used to measure the amount of target protein BMP4 that was produced by transfected cells and to assess the effect of non-viral transfection on the migration, invasion, and differentiation characteristics of hAMSCs (Scheme 1B). The ability of NP-transfected hAMCSs to migrate towards brain tumors was evaluated *in vivo* after systemic and local administration (Scheme 1C). Finally, hAMSCs engineered to express BMP4 were shown *in vivo* to have a significant effect on survival in a human primary malignant glioma model (Scheme 1D).

2.2. Polymer synthesis

PBAEs were synthesized using a two-step procedure, as previously described [44]. First, one diacrylate backbone diacrylate monomer (B3, B4, or B5) was combined with one amine sidechain (S3, S4, or S5) by conjugate addition at 90 °C for 24 h at a 1.1:1 or 1.05:1 acrylate-to-amine (B-to-S) molar ratio. Next, the resulting diacrylate-terminated neat B-S polymer was dissolved in anhydrous tetrahydrofuran (THF) and combined with end-cap amine-containing small molecules (E6 or E7) in anhydrous THF (Fig. 1). The final polymer solution was stirred for 1 h at room temperature, then precipitated into diethyl ether to remove solvents and unreacted small molecules. The polymer was collected and washed with excess ether. The ether was then decanted, and the polymer was dried under vacuum for 48 h. The neat polymer was then dissolved in anhydrous dimethyl sulfoxide (DMSO) at a concentration of 100 mg/mL and was stored at −20 °C until use.

The molecular weight of top polymers was measured by gel permeation chromatography (GPC; Waters, Milford, MA) in BHT-stabilized tetrahydrofuran with 5% DMSO and 1% piperidine.

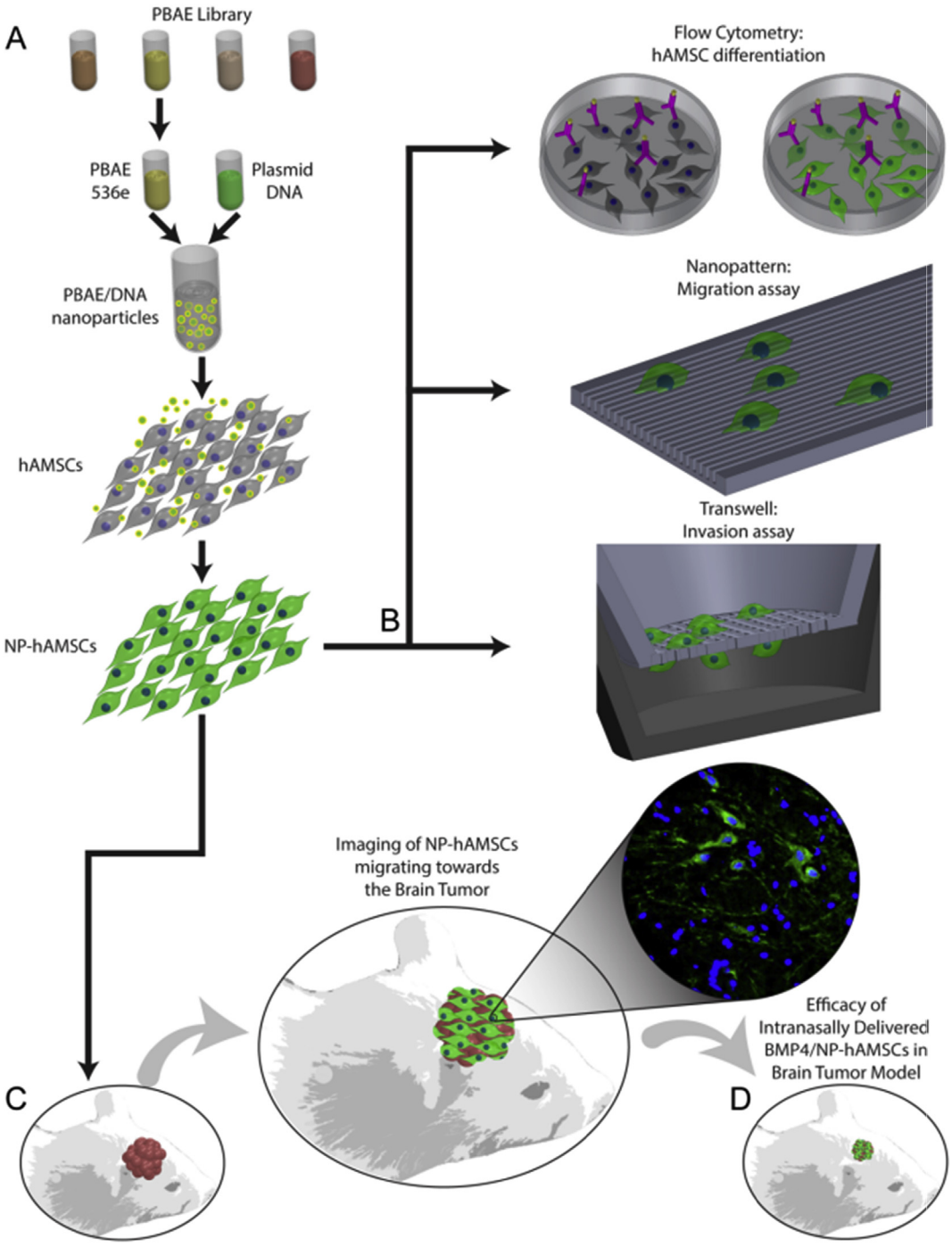

Scheme 1. Experimental design: graphical representation. (A) Human adipose mesenchymal stem cells (hAMSCs) were transfected with a PBAE library to identify the optimal formulations. (B) Functional assays were performed to verify the effect of non-viral transfection on the characteristics of hAMSCs. (C) The ability of NP-hAMCSs to migrate towards the brain was evaluated *in vivo* after systemic administration. (D) Intranasally delivered BMP4-producing NPs significantly extend survival in glioma model.

Number-averaged and weight-averaged molecular weights (M_n and M_w, respectively) were calculated using polystyrene standards (Fig. 2).

2.3. In vitro cell culture

All hAMSCs used were StemPro® Human Adipose-Derived Stem Cells purchased from Life Technologies (formerly Invitrogen, Carlsbad, CA) and were grown in complete Mesenpro RS medium (2% serum) with 1% penicillin/streptomycin (Mediatech) and 1% GlutaMAX (Invitrogen). Cells were grown to 80% confluence before each passaging. For all *in vitro* and *in vivo* experiments, hAMSCs were used at passage 4.

Commercial U87 human malignant glioma cells were purchased from ATCC (Manassas, VA) and grown in Dulbecco's modified Eagle's medium (DMEM) (Life Technologies) with high glucose, supplemented with 10% fetal bovine serum (FBS; Gemini Bioproducts Inc.) and 1% penicillin-streptomycin (Mediatech Inc.).

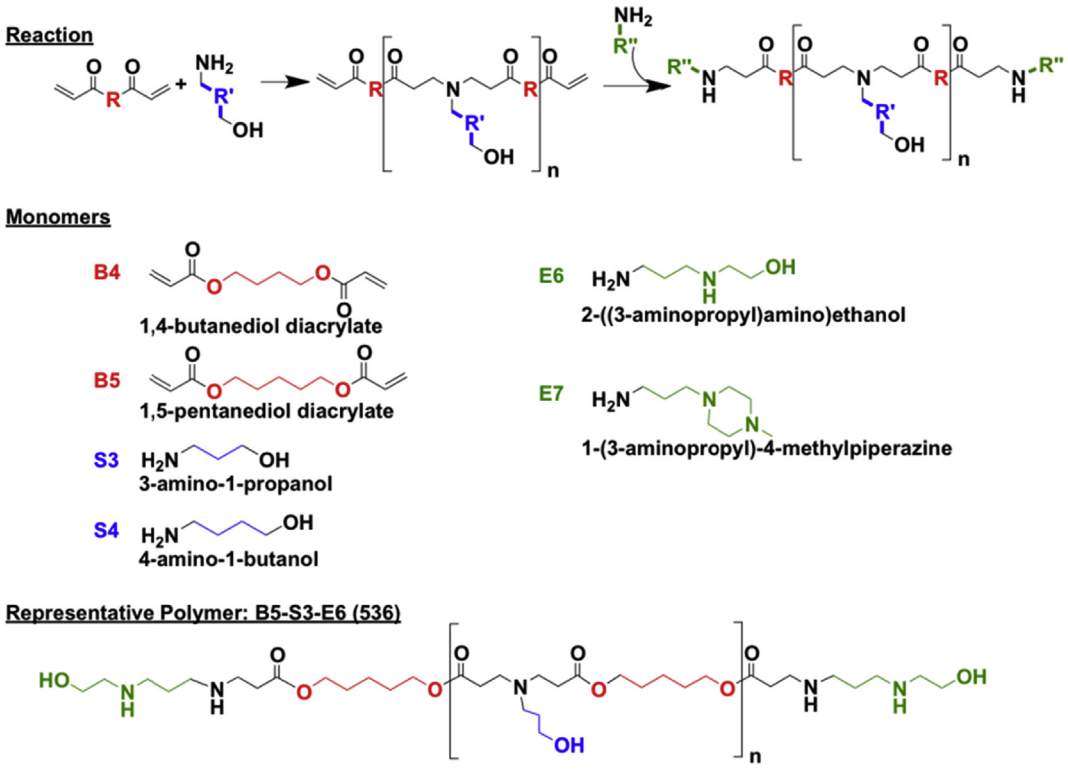

Fig. 1. Schematic illustration of PBAE synthesis. For each polymer, one backbone monomer (B) is polymerized with one sidechain (S) and functionalized with one end-cap (E) monomer. The structure of polymer B5-S3-E6 (536) is shown as an example.

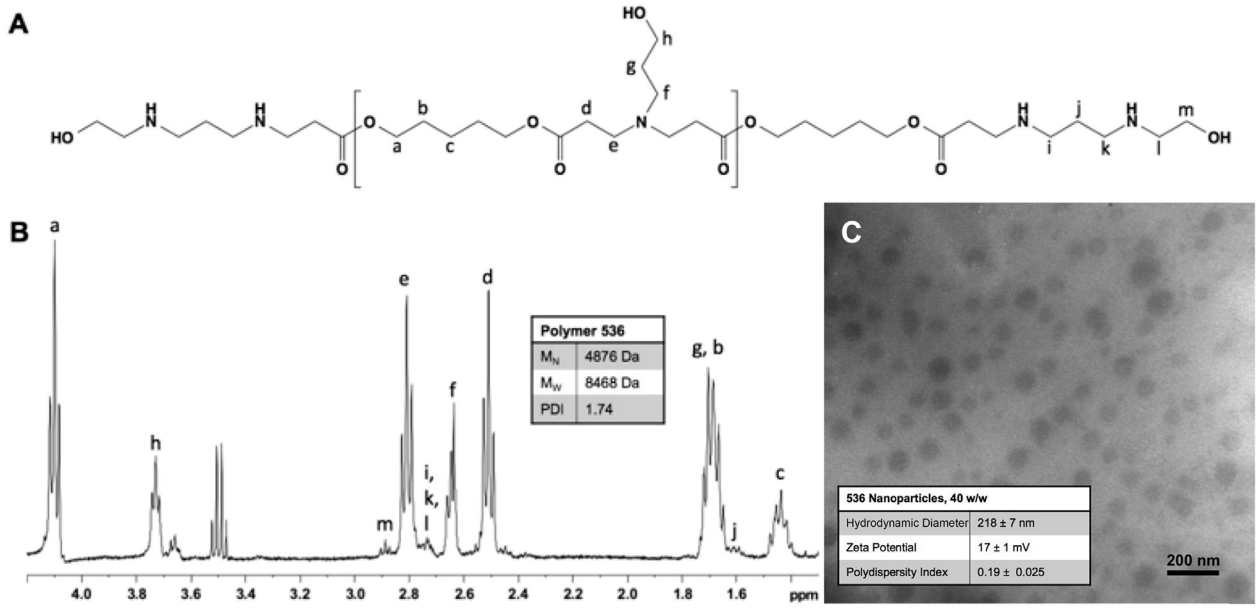

Fig. 2. Characterization of polymer 536e, 1.1:1 and nanoparticles at 40 w/w. (A) Proton peaks are labeled with letters corresponding to protons along the structure of 536. (B) ^{1}H NMR spectrum of polymer 536e, 1.1:1 ($CDCl_3$, 400 Hz). Gel permation chromatography (GPC) analysis of 536e, 1.1:1. The table indicates the number-averaged (M_N) and weight-averaged (M_W) molecular weight and polydispersity index (PDI). (C) TEM imaging of 536 nanoparticles shows nanoparticles of the same size and morphology (scale bar = 200 nm). Nanoparticle hydrodynamic diameter and zeta potential are reported as acquired via DLS.

Human primary BTIC oncosphere culture 0913 (GBM1a) was originally derived by Vescovi and colleagues and cultured in serum-free DMEM/F-12 (Life Technologies) supplemented with EGF/βFGF [45]. All cells were grown at 37 °C in a humidified incubator with 5% CO_2.

2.4. In vitro optimization of hAMSC transfection

For initial screening, hAMSCs were seeded in completed MesenPro RS medium at 10^4 cells/cm^2 in 96-well plates and allowed to adhere overnight. The next day, eGFP DNA was diluted to 0.12 mg/

mL in 25 mM sodium acetate pH 5 buffer (NaAc). Polymer-to-DNA mass ratios from 20 to 67.5 w/w were tested (2.4–8.1 mg/mL polymer diluted in 25 mM NaAc was mixed with 0.12 mg/mL DNA in NaAc at a 1:1 vol ratio). The resulting mixture was mixed by pipetting and incubated at room temperature for 10 min to allow the nanoparticles to form for self-assembly. Because PBAEs are known to completely entrap DNA under these complexation conditions and within the range of weight-to-weight ratios used here [41,46], no further steps were needed to purify the resulting nanoparticles from free DNA. The PBAE/DNA nanoparticles were then added to cells at a 1:5 volumetric ratio of nanoparticles to medium, with a final DNA dose of 10 μg/mL for all polymer treatment groups. After 1.5 h of incubation, all particles and media were removed, the cells were washed with 1xPBS to remove residual particles, and complete Mesenpro RS medium was replaced in the wells. After 48 h, cells were trypsinized and transferred to round-bottom 96-well plates in 1xPBS with 2% fetal bovine serum (FBS). eGFP expression was measured by flow cytometry using an Accuri C6 flow cytometer with an Intellicyt high-throughput loader. Reported values are the percent of GFP^+ cells calculated using the signal from the FL1 detector (emission: 530/30 nm). The MTS assay (CellTiter Aqueous One, Promega, Madison WI) was used according to the manufacturer's protocols to assess cell viability.

For the leading polymer, the transfection protocol was further optimized to find the optimal dose for high transfection rate and low toxicity over time for large-scale transfections. hAMSCs were seeded at 10^4 cells/cm^2 in 200 μL/cm^2 medium and allowed to adhere overnight. PBAE/DNA nanoparticles were prepared as above, and varying volumes were added to the media for 1.5 h before being replaced with fresh medium as above. Transfection efficacy was measured over time by flow cytometry. Cell viability over time was measured by passaging the cells, re-seeding at a known cell number, and doing MTS assay the next day. The viability was calculated by normalizing the MTS signal to that from non-transfected cells, also passaged and re-seeded at the same cell density. The final nanoparticle-to-medium ratio used for the rest of the study was 150 μL nanoparticles/mL medium, with a final DNA dosage of 6.67 μg/mL (Fig. S2). Cells transfected with eGFP DNA were referred to as GFP/NP-hAMSCs; those transfected with BMP4 were referred to as BMP4/NP-hAMSCs.

For testing of the commercial Lipofectamine™ 2000 control, cells were seeded in 24-well plates at 10^4 cells/cm^2 in 400 μL medium and allowed to attach overnight. Reagents were formulated as specified by the manufacturer at a ratio of 2.5 μL Lipofectamine to 1 μg DNA and a final concentration of 15 μg DNA/mL in Opti-MEM I (Life Technologies). The formulation was added to hAMSCs at final DNA doses between 0.6 μg/mL and 2.5 μg/mL. Higher doses were not tested because of the excessive toxicity seen within this range. Cells were incubated with Lipofectamine/DNA and then analyzed for viability and transfection efficacy as described above. The final dose of 1.05 μg/mL was used as a control in further studies, being the highest dose that caused <50% cell death and achieved >15% transfection efficacy (Supplementary Fig. S1).

2.5. Sphere-forming assays

BTICs (2.5×10^3) were seeded in triplicate in low-adhesion T-25 tissue culture flasks (2.5×10^5 cells/well) in sphere-promoting media as previously described [47] and treated with 20 μL/ml of concentrated conditioned media conditioned from culture with non-transfected hAMSCs (CM-Control), GFP/NP-AMSCs (CM-GFP), or BMP4/NP-hAMCs (CM-BMP4). The presence of spheres (3D multicellular structures greater than 50 μm in diameter [48]) was assessed by light microscopy after 14 d. Fifty pictures of each flask were taken using a Zeiss Microscope Axio-Observer.Z1. Then the largest cross sectional diameter and number of neurospheres formed for the three different experimental groups were measured using MATLAB, and the total number of spheres per FOV was summed.

2.6. In vitro evaluation of hAMSC behavior

2.6.1. In vitro invasion assay

The invasion capacity of nanoparticle-transfected hAMSCs was evaluated through a standard transwell migration assay using a transwell polycarbonate filter (8 μM pore size) (Corning Inc, Lowell, MA). Non-transfected hAMSCs, BMP4-secreting hAMSCs transduced with lentivirus, and BMP4-secreting hAMSCs transfected with nanoparticles were plated in the upper chamber of a 24 transwell plate at 3×10^4 cells/well in complete Mesenpro medium. Complete Mesenpro medium with additional 2% FBS was used to culture U87 human malignant glioma cells to 90% confluence, and this conditioned medium was used as a chemo-attractant in the lower chamber. The cells were cultured for 24 h at 37 °C. The cells that had not migrated were removed from the upper face of the filters using cotton swabs, and those that migrated to the underside of the upper chambers were stained with Diff-Quik Staining Set (Siemens). Nine pictures, taken from preset coordinates to cover the entirety of the well, were taken automatically by a Zeiss Microscope Axio-Observer.Z1, and the cells were counted using ImageJ software. All conditions were conducted in triplicate and repeated in two separate experiments.

2.6.2. Nanogrooved pattern cell migration assay

The migration of NP-hAMSCs was quantified using a novel directional migration assay using nano-ridges/grooves constructed of transparent poly(urethane acrylate) (PUA) and fabricated using UV-assisted capillary lithography as previously reported [23,25,26,47,49–51]. Nanopattern surfaces were coated with laminin (3 μg/cm^2). Cell migration was quantified using timelapse microscopy (Supplementary Movie 1). Long-term observation was done on a motorized inverted microscope (Olympus IX81) [47,50,51] equipped with a Cascade 512B II CCD camera and temperature and gas controlling environmental chamber. Phase-contrast and epifluorescent cell images were automatically recorded under 10× objective (NA = 0.30) using the Slidebook 4.1 (Intelligent Imaging Innovations, Denver, CO) for 15 h at 10–20-min intervals. A custom-made MATLAB script was used to identify cell boundaries from phase-contrasted images and to measure cell centroid positions. Average individual cell speed was calculated based on individual cell trajectories and duration of image acquisition. Mean of distance, speed, and displacements at various time intervals were calculated using a previously published method. For each condition, over 100 cells were quantified in total. All conditions were conducted in triplicate and repeated in three separate experiments.

Supplementary video related to this article can be found at http://dx.doi.org/10.1016/j.biomaterials.2016.05.025

2.7. Animal procedures

Athymic female rats weighing 150–200 g were purchased from Harlan Bioproducts 160–200 g (Indianapolis, IN). All animals were treated in accordance with the policies and guidelines of the Johns Hopkins University Animal Care and Use Committee. All rats were housed in standard facilities and provided free access to rodent chow and Baltimore City water.

All surgical procedures were performed using standard sterile techniques. Rats were anesthetized before surgery with an intraperitoneal (IP) injection of 3 mL/kg of a stock solution containing

75 mg/mL ketamine hydrochloride (Ketathesia, Butler Animal Health Supply; Dublin, OH); 7.5 mg/mL xylazine (Lloyd Laboratories; Shenandoah, Iowa), and 14.25% ethyl alcohol in 0.9% NaCl.

2.8. Intracranial tumor inoculation

The intracranial xenografts were established as previously described [52]. The rats were anesthetized, and their heads were shaved with clippers and prepared with alcohol and Prepodyne solution (West Penetone, Montreal, Canada). A midline scalp incision was made, exposing the sagittal and coronal sutures. With the use of an electric drill with a 2-mm round cutting burr, a small hole was made in the skull centered 3 mm left to the sagittal suture and 4 mm posterior to the coronal suture. Care was taken to avoid the superior sagittal sinus. The animals were placed in a stereotactic frame, and 1×10^6 U87 cells or 5×10^5 BTICs (GBM1a) were injected over 3 min via a 26-gauge needle inserted to a depth of 3.5 mm at the center of the burr hole into the rat's striatum. After tumor cell inoculation, the needle was removed, the site was irrigated with normal saline, and the incision was closed with surgical staples.

2.9. Administration of NP-hAMSCs

The hAMSCs were injected 2 days post-transfection based on *in vitro* transfection efficacy and viability results. The animals were re-anesthetized 10 days after tumor implantation using the anesthetic regime described above. For intranasal (IN) administration, the anesthetized animals were placed in a supine position, and the nasal cavity of each animal was treated with 5 repeated inoculations at 5 min intervals in alternate nostrils (5 μL in each nostril), with a total of 2×10^6 NP-AMSCs administered in 50 μL sterile PBS [16]. For systemic injection (IV), the rats were not anesthetized. The same number of NP-hAMSCs was injected into the tail vein in a volume of 600 μL sterile PBS as previously described [53].

2.10. In vivo NP-AMSC tracking: fluorescence imaging of GFP/NP-hAMSCs

U87 cells were injected into rats as described above to establish an orthotopic tumor. Twelve days after tumor inoculation, hAMSCs were transfected with GFP DNA using PBAE 536, 1.1:1 according to the protocols above. Two days after transfection, GFP/NP-hAMSCs were administered to rats IV and IN as described above. U87 bearing rats injected intracranially with non-transfected hAMSCs were used as background controls. Three days after administration of cells, the animals were euthanized and perfused with 4% paraformaldehyde, and brains were extracted for measurement with IVIS (Caliper Life Sciences, formerly Xenogen). Images were recorded with an exposure time of 5 min. Signal was recorded as photon counts using Xenogen IVIS 200 system using the GFP filter set. Image analysis was done using Living Image software (Perkin Elmer).

2.11. Histological analysis

After perfusion and IVIS imaging, the brains of U87-bearing rats injected with GFP/NP-hAMSCs were preserved in formalin and processed for histological analysis. Ten-micron slices were cut within 1 mm of the tumor injection site and. The sections were first imaged directly under confocal microscopy and then stained for DAPI and human nuclei as previously described [47] and imaged using a fluorescence microscope (AxioObserver Z1, Zeiss).

2.12. Survival of tumor-bearing rats after treatment with BMP4/NP-hAMSCs

BTIC tumors were established in seventeen athymic rats as described above. BMP4/NP-hAMSCs were injected IN 7 and 14 days after tumor inoculation, as described above in the treatment animals, and GFP/NP-hAMSCs were injected for the control animals. Survival of the rats was monitored for 20 days.

2.13. Statistical analysis

Statistical analysis was performed using GraphPad Prism 6. It consisted of One-way ANOVA with Bonferroni or Tukey post-tests or a non-parametric Kruskal-Wallis test, depending on the type of distribution of the data. Data distribution was determined using the D'agostino test; graphs represent the mean ± SEM. For survival studies, survival was analyzed using the Kaplan-Meier estimator, and statistical significance was established using log-rank analysis.

3. Results and discussion

3.1. Safe and effective non-viral transfection of hAMSCs via biodegradable PBAE nanoparticles

Despite encouraging preclinical studies, clinical translation of MSC-based therapies for the treatment of brain cancer has been limited by a number of factors, including the use of viruses in traditional gene transfer technologies. The risks of insertional mutagenesis, excessive inflammation and immune response, and toxicity associated with viruses are significant hurdles for the clinical application of therapies based on genetically engineered cells [54–56]. Only a limited number of studies have been conducted using non-viral vectors for gene delivery to MSCs for cell-based therapies, particularly in primary human cells. PBAEs have been shown by our group and others to have promise for transfection of human cells [41,42,44], including hAMSCs [57], even though hAMSCs have previously been demonstrated to have low non-viral transfection efficiencies compared to other human cell types [43]. Here, we engineered PBAE/DNA NP formulations for effective transfection of hAMSCs (Scheme 1). A library of purified poly(beta-amino ester)s (PBAEs) was synthesized as previously described [44] (Fig. 1) and screened to identify the polymer with the least cytotoxicity on hAMSCs. Among those, the PBAE designated 536, 1.1:1 (Fig. 2), mixed with DNA at a 40:1 ratio by mass (40 w/w) was found to be the leading formulation, with high transfection efficacy as measured by flow cytometry (75 ± 2% positive cells) and cell viability (71 ± 7%) (Fig. 3A, B). The nanoparticles in this formulation were found ($n = 3$ independently prepared samples) to have a hydrodynamic diameter of 218 ± 7 nm, a polydispersity index (PDI) of 0.19 ± 0.03, and a positive zeta potential of 17 ± 1 mV (Fig. 3C).

For comparison, a leading and well-published commercially available transection reagent, Lipofectamine™ 2000, was optimized for use in hAMSCs according to the manufacturer's instructions (Supplementary Fig. S1) to establish protocols that would maximize its efficacy while minimizing its adverse side effects. With a maximum transfection efficacy of 16 ± 3% for Lipofectamine™ 2000 formulations that showed <50% toxicity, Lipofectamine™ 2000 was significantly less effective at transfection than our optimized PBAE nanoparticles ($p < 0.0001$) and presented unacceptable levels of cytotoxicity in hAMSCs (Fig. 3C). Because of its high toxicity (>80% toxicity at 2.5 μg/mL DNA doses, Supplemental Fig. S1), Lipofectamine™ 2000 was not used as a control at the same dosage as that used for PBAEs (6.67 μg/mL), as this would have underrepresented the efficacy of the commercial

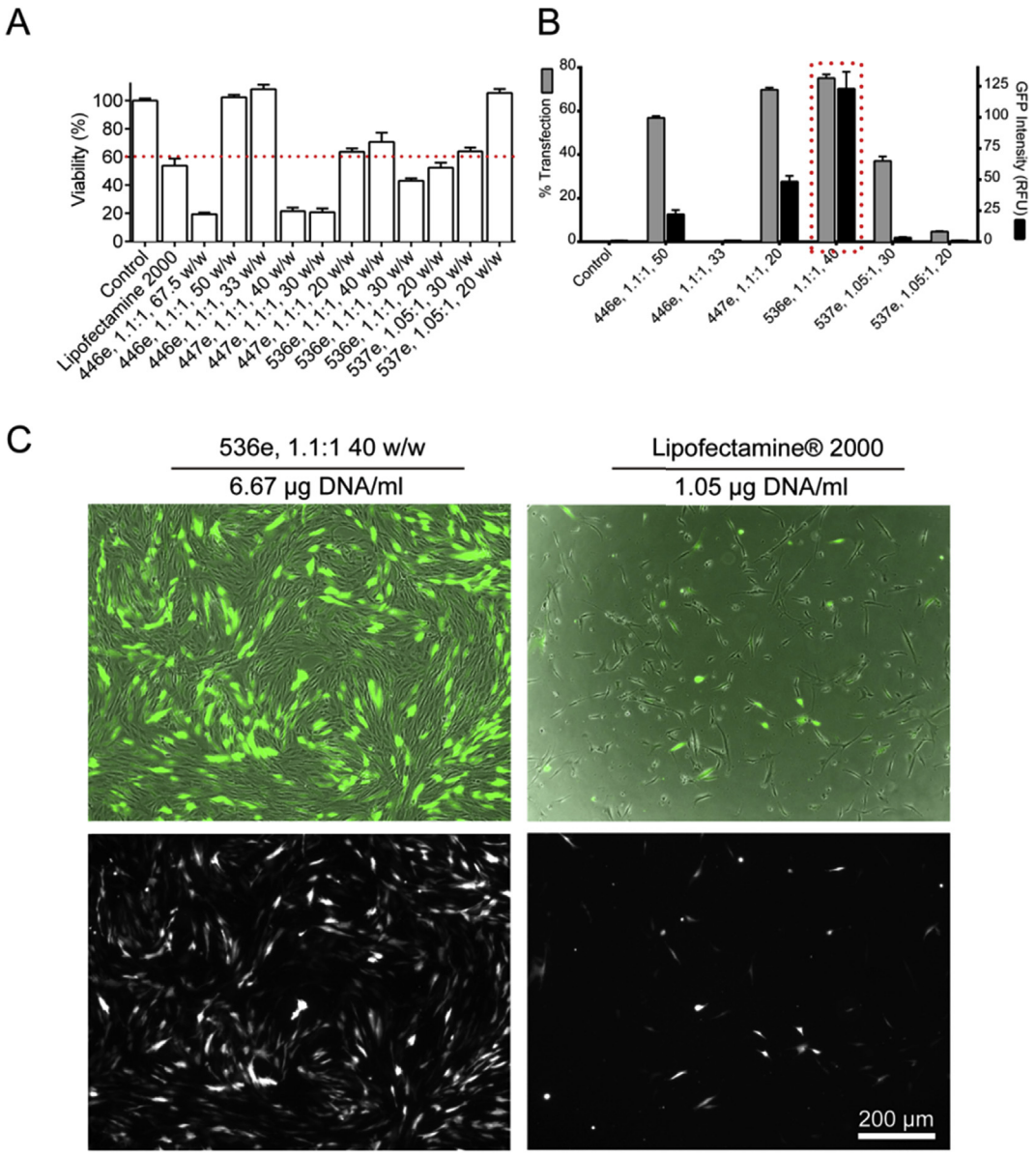

Fig. 3. PBAE nanoparticle formulations were optimized for high hAMSC transfection and viability. (A) Viability of cells treated with the top PBAE nanoparticle formulation and commercially available Lipofectamine™ 2000 was measured as the relative metabolic activity of treated cells normalized to that of untreated cells. (B) Transfection efficacy of formulations with high (>60%) cell viability was measured as percent of cells expressing GFP and geometric mean fluorescence intensity normalized to untreated cells. (C) Fluorescence microscopy clearly shows that the top PBAE formulation was significantly superior to the optimized formulation of Lipofectamine™ 2000 in safety and transfection capacity ($p < 0.0001$). Bar graphs show mean ± SEM.

reagent due to high cell death. The Lipofectamine™ 2000 formulation ratio and dosage were independently optimized following the manufacturer's instructions. Each material was compared at its own optimized formulation. The biodegradable linkages of the PBAEs minimize cytotoxicity, which has been shown to be affected by molecular weight of the polymer [58,59], and the polymer structure optimization process we used here for polymer selection ensured that we found the most effective PBAE structure for gene delivery to this specific cell type. Hence, experiments were carried out with an optimized dosage of PBAE 536, 1.1:1 nanoparticles as the gene delivery agent (Supplementary Fig. S2).

The duration of transgene expression and viability of hAMSCs after transfection with PBAE/DNA NPs were assessed over time. hAMSCs transfected with PBAE particles containing GFP DNA (GFP/NP-hAMSCs) showed an initial decrease in viability within the first 24 h but had completely recovered 48 h after transfection (no significant difference from 100%) (Fig. 4A). GFP/NP-hAMSCs were also shown to express GFP in at least 70% of cells for 5 days, with 60% of cells still GFP^+ after 7 days (Fig. 4B, C). To our knowledge, this represents higher levels of gene delivery to hAMSCs than have been previously reported using alternative PBAE structures or any other polymeric nanoparticle delivery system.

3.2. *Efficacy of BMP4-producing NP-hAMSCs on human primary glioma cell lines*

To investigate if NP-hAMSCs could be successfully used to deliver a therapeutic gene of interest, we used the leading PBAE 536, 1.1:1 to genetically engineer the hAMSCs to express bone morphogenetic protein 4 (BMP4), a growth factor known to reduce

the clonogenic ability of BTICs in human malignant gliomas. hAMSCs transfected with BMP4 nanoparticles (BMP4/NP-hAMSCs) showed over 24,000-fold higher mRNA expression levels than untreated hAMSCs 24 h after transfection (Fig. 5A). The difference in the BMP4 and GFP mRNA expression levels is likely due to differences between the two plasmids used; however, both plasmids do lead to much higher expression of the target gene in transfected cells compared to that in controls. Furthermore, BMP4 was secreted into the culture medium, with a Western blot showing that 10^6 transfected cells produced approximately 52.5 ng of BMP4 over 72 h (Fig. 5B). This is similar to the amount of BMP4 that we found in a previous study to be secreted in the same timeframe by hAMSCs transduced by a lentivirus (74 ng BMP4 over 3 days) [23].

Next, we investigated the *in vitro* effect of BMP4 released from BMP4/NP-hAMSCs by assessing the sphere-forming capacity (SFC) of BTICs upon treatment with conditioned media (CM) from the hAMSCs as previously described [60]. The SFC of BTICs treated with CM derived from GFP/NP-hAMSCs (CM-GFP) was not significantly different from that of BTICs treated with non-transfected hAMSCs (CM-Control). However, those treated with CM derived from BMP4/NP-hAMSCs (CM-BMP4) had significantly impaired SFC compared to the controls with both the number and diameter of spheres being significantly less than the controls (62 ± 11% fewer spheres and 72 ± 7% lower diameter than controls, $p < 0.005$ and 0.0001, respectively) (Fig. 5C–E). These data show for the first time that non-virally transfected hAMSCs can be engineered to produce biologically active BMP4.

3.3. Functional capacity of nanoparticle-transfected hAMSCs vs. virally transduced hAMSCs

In order for hAMSCs to be used as targeted drug delivery vehicles for glioblastoma therapy, the processes used to modify them must allow them to maintain their normal behavior, including their

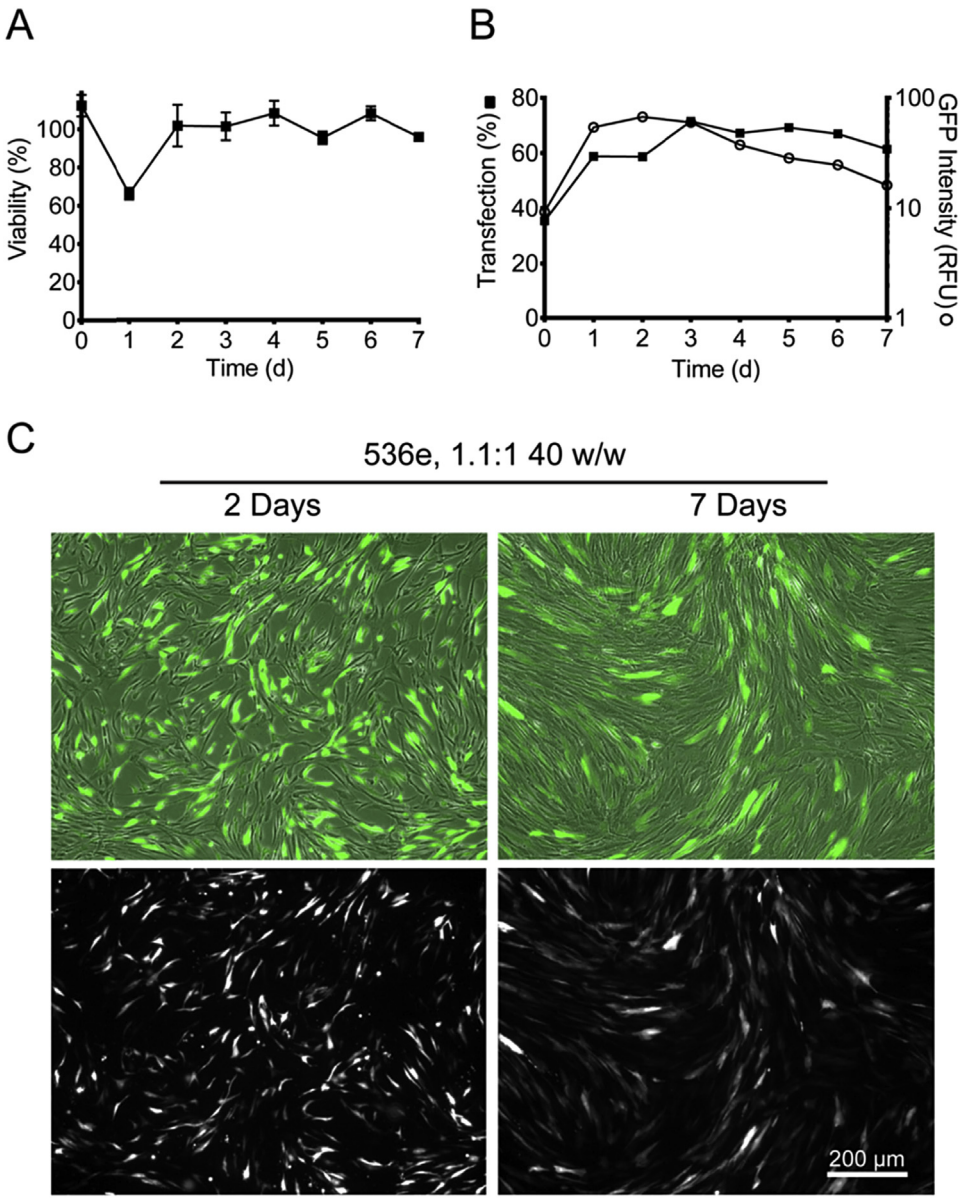

Fig. 4. PBAEs safely and effectively transfect hAMSCs with high transgene expression over time. (A) Cell viability over time was measured by MTS assay. (B) Transfection efficacy over time measured by flow cytometry and is reported as the percent of cells GFP^+ (solid squares) and the geometric mean GFP intensity per cell (open circles). Each data point represents the mean ± SEM of three points. (C) Fluorescence microscopy of hAMSCs 2 and 7 days after transfection.

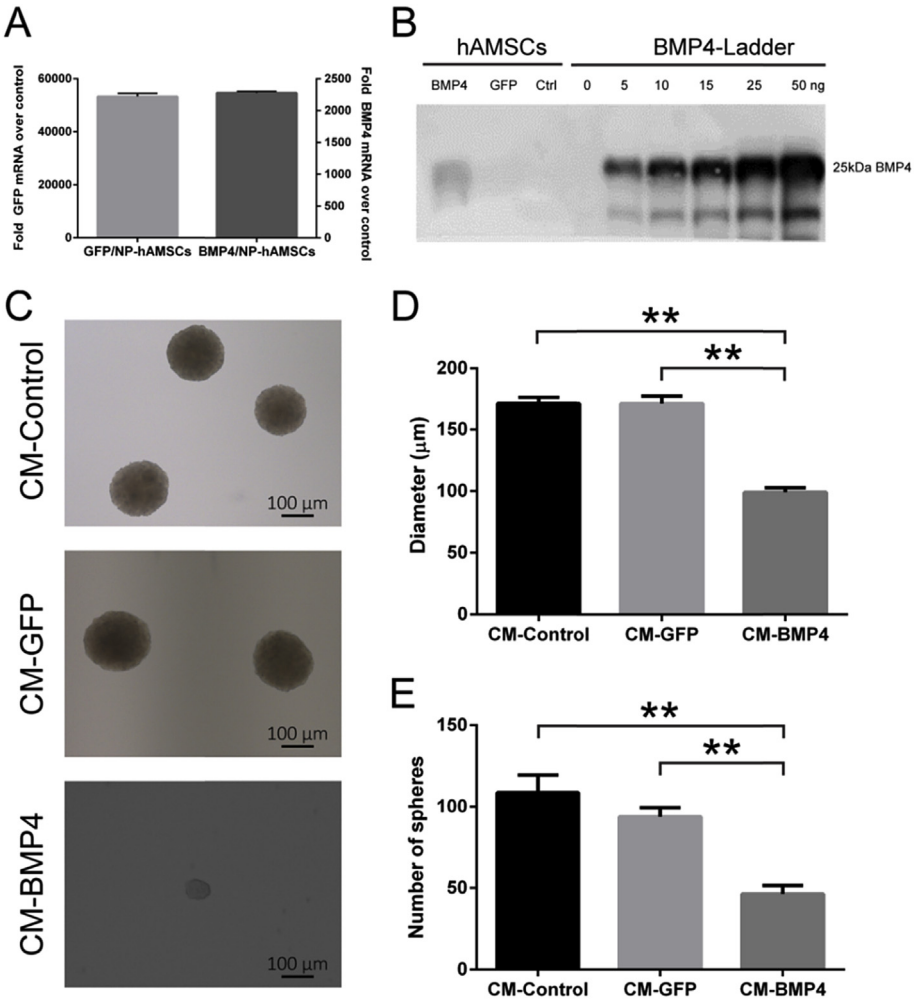

Fig. 5. BMP4/NP-hAMSCs express and secrete BMP4 *in vitro* and decrease BTIC clonogenic potential. (A) Quantitative PCR shows high mRNA expression of eGFP or BMP4 in hAMSCs transfected with eGFP or BMP4, respectively, within the first 24 h after transfection. (B) Western blot shows the amount of BMP4 secreted by 1.4×10^4 hAMSCs in the 72 h after transfection, equivalent to 52.5 ng BMP4 per 10^6 hAMSCs. (C) Representative images of neurospheres treated with concentrated conditioned media (CM) obtained from non-transfected hAMSCs (CM-Control), GFP/NP-hAMSCs (CM-GFP) and BMP4/NP-hAMSCs (CM-BMP4). (D,E) Sphere-forming capacity was significantly reduced in the BTICs exposed to BMP4 from transfected hAMSCs. Bar graphs show mean ± SEM from three independent experiments performed in triplicate. $^{**}p < 0.0001$.

multipotency and their capacity for migration and invasion. Therefore, we used flow cytometry analysis to compare cell surface marker expression in BMP4/NP-hAMSCs and non-transfected hAMSCs (Fig. 6A). There was no significant difference between the transfected and untreated cells, indicating that transfected hAMSCs remained undifferentiated and retained their multipotency. In addition, *in vitro* functional assays were used to compare non-transfected hAMSCs with hAMSCs genetically engineered to produce BMP4 via either NP transfection or lentiviral transduction. Although BMP4/NP-hAMSCs showed 20–25% reduction in migration speed and distance and invasion compared to untreated cells, the nanoparticle-transfected hAMSCs were significantly better ($p < 0.005$) in all parameters of migration and invasion than hAMSCs transduced with lentivirus (BMP4/LentiV-hAMSC, Fig. 6B, C, Movie S1). Given the wide range of potential applications of hAMSCs as delivery vehicles, these data provide encouraging information on the effects of non-viral vectors on hAMSCs' functional capacities.

3.4. Brain homing efficacy of nanoparticle-transfected hAMSCs after systemic administration in a human glioma model

In order to test the ability of NP-transfected hAMSCs to migrate toward a brain tumor *in vivo*, hAMSCs were transfected with GFP DNA (GFP/NP-hAMSCs) and injected either intranasally (IN) or intravenously (IV) into human glioma tumor-bearing rats (Fig. 7A). The localization of injected NP-hAMSCs was visualized using a Xenogen *In Vivo* Imaging System (IVIS) to measure fluorescence signal from excised brains (GFP/NP-hAMSCs). Three days after injection, high fluorescence signal above background autofluorescence was observed in the brains of rats treated with GFP/NP-hAMSCs either IN or IV (Fig. 7B). Specifically, the fluorescence signal of the left hemisphere, where the tumor had been implanted, was approximately 5-fold higher in the animals injected with GFP/NP-hAMSCs compared to the left hemisphere of the control rats injected with non-transfected hAMSCs (Fig. 7C). This indicates that the small degree of decreased mobility in transfected hAMSCs did not prevent them from being able to migrate to and accumulate at the tumor site in the brain after both intranasal and intravenous injection. Some hAMSCs were also found in the right hemisphere of the brain without a tumor, indicating that hAMSCs are able to cross

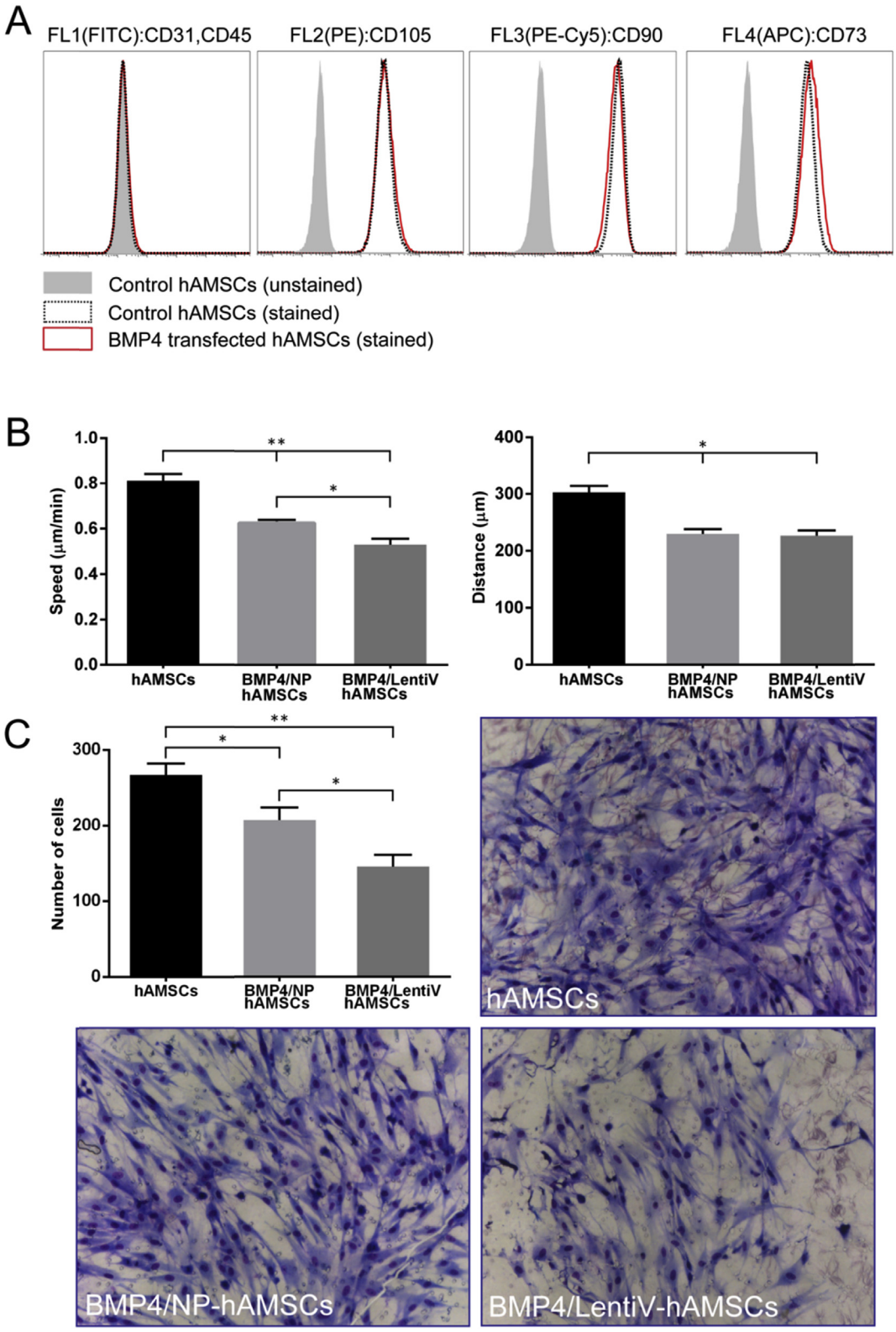

Fig. 6. NP-engineered hAMSCs retain functionality better than virus-engineered hAMSCs. (A) Expression of cell-surface markers of multipotency was measured by flow cytometry analysis in untreated and NP-hAMSCs. (B) Quantification of migration speed and distance of untreated hAMSCs (hAMSCs), BMP4-secreting hAMSCs genetically modified via nanoparticle (BMP4/NP- hAMSCs) or via lentiviral vector (BMP4/LentiV- hAMSCs) were evaluated on a nanopatterned substrate by a 15 h timelapse. (C) Quantification and representative images of transwell invasion assays were performed by exposing untreated hAMSCs, NP-transfected, and LentiV-transduced hAMSCs to conditioned U87-derived media. Each bar is the mean ± SEM of two independent experiments performed in triplicate, $^{*}p < 0.005$, $^{**}p < 0.0001$.

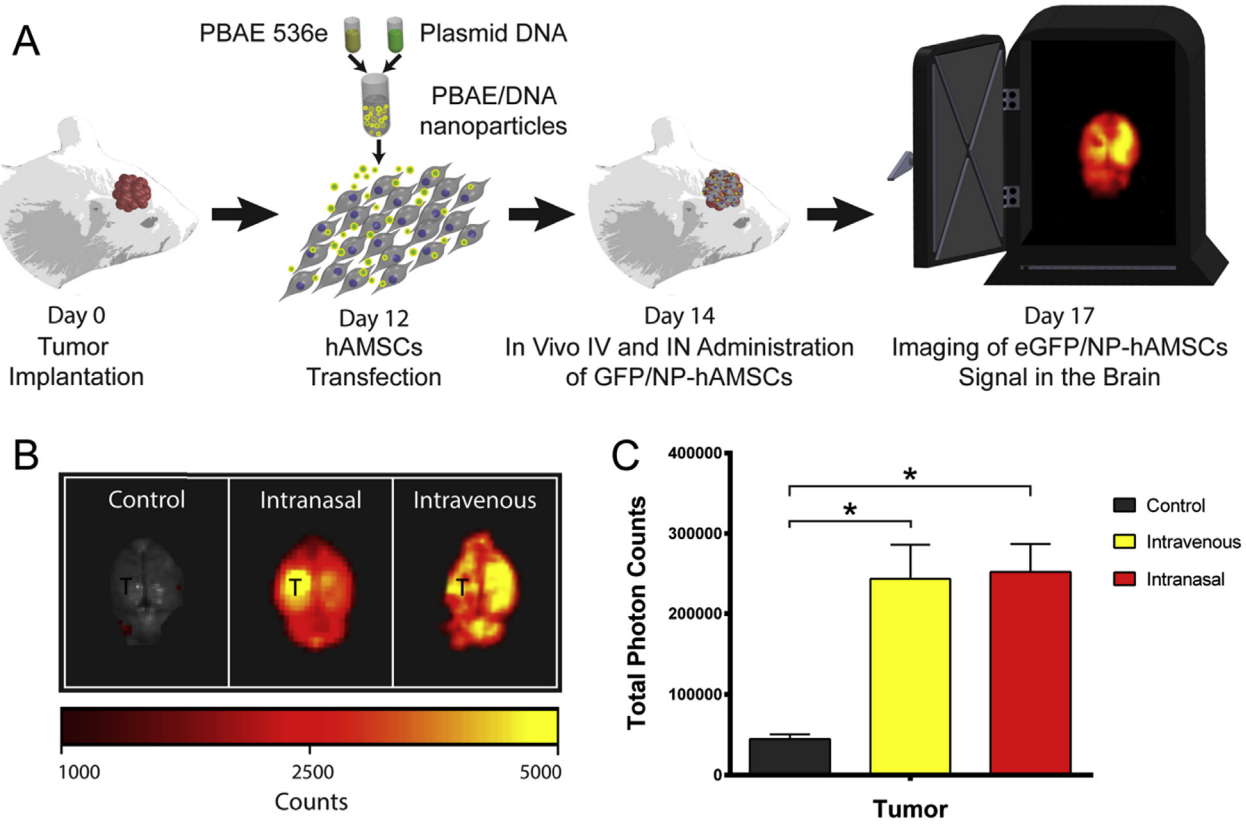

Fig. 7. NP-hMSCs show brain-homing tendencies after intranasal and intravenous administration in a human glioma model. (A) hAMSCs engineered with GFP DNA nanoparticles (GFP/NP-hAMSCs) were administrated intranasally (IN) and intravenously (IV) in athymic rats orthotopically implanted with human glioma. The fluorescence signal of the brains of the control animals and animals treated with GFP/NP-hAMSCs was then measured by IVIS. (B) Representative images of the brains of control rats and rats treated with eGFP/NP-hAMSCs brains 3 days after the IN or IV administration of the hAMSCs (T = tumor injection side). (C) Quantitative analysis of GFP signal of the left hemisphere (T) of control and eGFP/NPhAMSCs-given animals. Data are presented as mean + SEM of two independent experiments (n = 3/group) *p < 0.005.

even an intact blood-brain barrier; however, in all animals, the signal found in the left hemisphere was statistically significantly higher or statistically equivalent to that found in the right hemisphere. Immunofluorescence staining and confocal microscopy confirmed the presence of the GFP/NP-hMSCs within the tumor tissue of these animals after intranasal administration (Supplementary Fig. S3).

Although malignant brain cancer can be targeted with local therapy, reaching the tumor site would necessitate surgery for each administration [61–64]. hAMSCs are an appealing vehicle for systemic delivery, as their tumor-homing capacity has been well-documented [26,65], they can be harvested from autologous sources in large quantities without patient comorbidity [66], and their lack of immunogenicity protects them from premature clearance by the immune system [67]. Previous studies have shown that injected hAMSCs do reach the site of the brain tumor and survive *in vivo* long enough to deliver their payload over days. However, their numbers decline sharply to undetectable levels after 14 days [23], alleviating potential concerns about their extended survival. Furthermore, hAMSCs can be cultured and modified *in vitro* for use as a "Trojan horse" of sorts, carrying a therapeutic payload to the tumor site. Other studies have shown that they can reach the brain tumor after intranasal administration [16] or reach site of cerebral ischemia after intravenous administration [23]. Our studies here demonstrate that a new chemical approach using synthetic nanoparticles to engineer hAMSCs while retaining their ability to migrate past various biological barriers in order to reach the tumor site.

3.5. Nanoparticle-transfected hAMSCs extend survival in a brain tumor model in vivo

To investigate the effect of BMP4-secreting hAMSCs on survival, primary humans BTICs were stereotactically implanted into the left striatum of athymic rats. BMP4/NP-hAMSCs were administered IN 7 and 14 days after tumor implantation (Fig. 8A). While 56% of control animals died within 14 days, BMP4/NP-hAMSC-treated animals survived significantly longer, with over 60% still alive after 16 days (21.4% increase in median survival time, $p = 0.02$) (Fig. 8B). These data indicate that BMP4 secreted by hAMSCs was not only able to suppress the tumorigenic potential of BTICs *in vitro* but was also able to significantly improve survival *in vivo*. Although the survival benefit is modest in absolute terms, the difference in median survival is significant, both mathematically and when considering the extremely fast course of disease in this aggressive glioma model from tumor inoculation to death in the untreated animal. For human patients with glioblastoma, median survival is approximately 15 months, and, assuming that this 21.4% increase in median survival is carried into the clinic, this could mean an estimated increase of 3.2 months in median survival for these patients. It is also important to note that the model here used consists of only BTICs, the chemo- and radio-resistant cells responsible for the self-renewal of the tumor, while clinical glioblastoma is in fact a heterogeneous tumor in which BTICs represent only part of the tumor cell population, with other cell populations having better sensitivity to conventional therapy. This improvement in survival could produce an important therapeutic effect in a clinical scenario, as

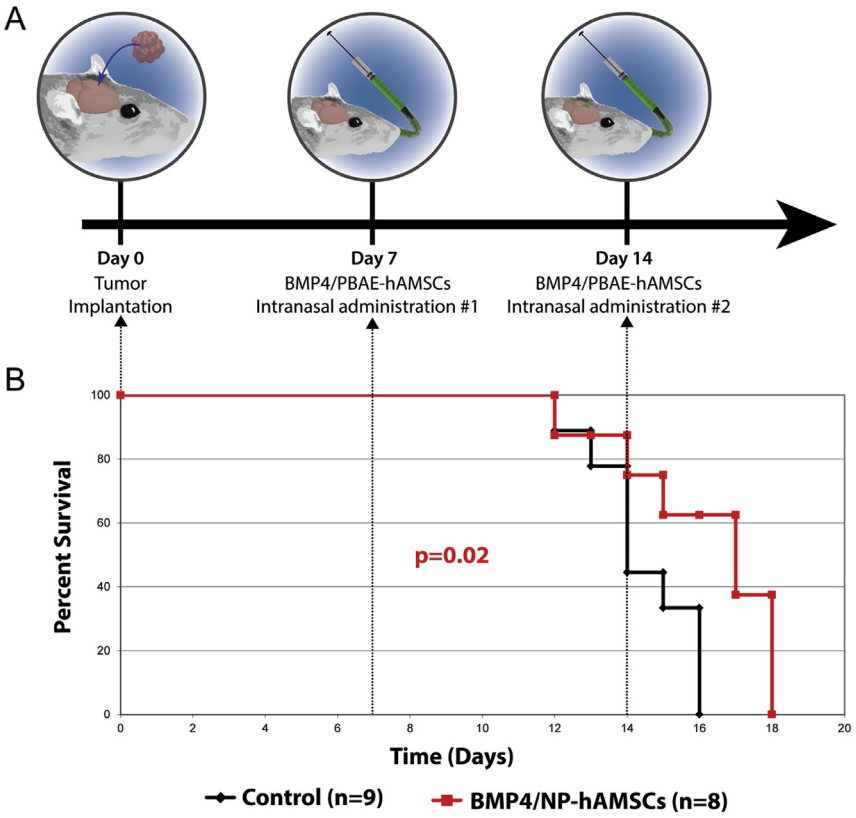

Fig. 8. Intranasally delivered BMP4/NP-hAMSCs extend survival in a brain tumor model *in vivo*. (A) Schematic representation of the *in vivo* study. The BTIC-derived glioma-bearing rats were treated with IN administration of BMP4/NP-hAMSCs on day 7 and day 14. (B) Kaplan-Meier plots of athymic rats that were implanted with primary human BTICs treated with GFP/NP-hAMSCs (Control, n = 9) or BMP4/NP-hAMSCs IN on day 7 and day 14 (n = 8). The median survival of the group receiving IN BMP4/NP-hAMSCs is significantly longer compared to that of the untreated control group (p = 0.02).

BTIC-targeting gene therapy can be combined with standard chemo- and radiotherapy to target the highly differentiated cells that constitute the bulk of the tumor. Moreover, due to the non-immunogenic nature of the hAMSCs used and because the synthetic nanoparticle components do not elicit a strong immune response as would a viral vector, multiple pulses of dosing were possible in this model. This is an important aspect of the technology, as it is after the second injection that significant differences in survival can be seen, and this could translate to multiple administrations of the therapeutic to a patient. The intranasal route to the brain tumor has recently proven effective for delivery of bone marrow-derived MSCs in murine preclinical models [16], but the number of cells that can reach the tumor site is limited (3–15%) [16,26]. It is therefore important that multiple injections be possible, and future studies will further explore the effect of multiple administrations of this therapy. Our experiments showed for the first time that the intranasal route can also be used for direct brain delivery of hAMSCs engineered with non-viral vectors, with significant improvement of survival *in vivo* when modified to express therapeutic protein BMP4.

In this study, we describe an *in vitro*, synthetic, non-viral nanomedicine approach to genetically engineer adult human stem cells, hAMSCs, with high efficacy and minimal loss in cell viability. We showed that the biodegradable polymer-based nanoparticle system can be used to induce production and secretion of BMP4 by hAMSCs with no change in differentiation state of the cells while also causing significantly less damage to the cells' migration and invasion capacities compared to the more commonly used viral transduction method. These engineered cells therefore retained their tumor tropism when injected non-invasively into rodent models, and, by delivering BMP4 to the target site of the brain tumor, the BMP4/NP-hMSCs were able to significantly improve survival of treated animals. This constitutes a safe and effective alternative to viral transduction for stem cell-based anti-glioma gene therapy and is first study showing the application of non-virally engineered hAMSCs for brain tumor therapy *in vivo*. In light of recent advances in stem cell-based therapy, an effective and safe non-viral transfection strategy for hMSCs may facilitate the utilization of MSC-based therapy clinically, with potential benefits for patients suffering a wide array of diseases.

Acknowledgment

JG and AQH were supported by NIH grants 5R01EB016721 and 1R01CA183827. SYT was supported by National Science Foundation Graduate Research Fellowship (DGE-1232825) and the Siebel Scholarship. KLK was supported by the NIH Cancer Nanotechnology Training Center (R25CA153952) at the JHU Institute for Nanobiotechnology, the Ruth L. Kirschstein NIH NRSA Predoctoral Fellowship (F31CA196163), and the ARCS Foundation. JK was supported by the Howard Hughes Medical Research Fellows. AV was supported by AIRC through grant #14368 IG 2013. Laboratory support (A.M., H.B., A.O., B.T.) from Mr. and Mrs. Joshua Fidler, Dr. and Mrs. Irving Sherman, and Mr. and Mrs. George Berry are also gratefully acknowledged.

Appendix A. Supplementary data

Supplementary data related to this article can be found at http://dx.doi.org/10.1016/j.biomaterials.2016.05.025.

References

[1] Q.T. Ostrom, H. Gittleman, P. Liao, C. Rouse, Y.W. Chen, J. Dowling, et al., CBTRUS statistical report: primary brain and central nervous system tumors diagnosed in the United States in 2007-2011, Neuro-Oncol. 16 (2014) 1–63.

[2] D.N. Louis, H. Ohgaki, O.D. Wiestler, W.K. Cavenee, P.C. Burger, A. Jouvet, et al., The 2007 WHO classification of tumours of the central nervous system (vol. 114, pg 97, 2007), Acta Neuropathol. 114 (2007) 547.

[3] K.L. Chaichana, P. Zadnik, J.D. Weingart, A. Olivi, G.L. Gallia, J. Blakeley, et al., Multiple resections for patients with glioblastoma: prolonging survival Clinical article, J. Neurosurg. 118 (2013) 812–820.

[4] K.L. Chaichana, H. Zaidi, C. Pendleton, M.J. McGirt, R. Grossman, J.D. Weingart, et al., The efficacy of carmustine wafers for older patients with glioblastoma multiforme: prolonging survival, Neurol. Res. 33 (2011) 759–765.

[5] M.J. McGirt, K.L. Chaichana, M. Gathinji, F.J. Attenello, K. Than, A. Olivi, et al., Independent association of extent of resection with survival in patients with malignant brain astrocytoma, J. Neurosurg. 110 (2009) 156–162.

[6] S.Y. Tzeng, J.J. Green, Therapeutic nanomedicine for brain cancer, Ther. Deliv. 4 (2013) 687–704.

[7] M. Blanchette, D. Fortin, Blood-brain barrier disruption in the treatment of brain tumors, Blood-Brain Other Neural Barriers Rev. Protoc. 686 (2011) 447–463.

[8] E.A. Nance, G.F. Woodworth, K.A. Sailor, T.Y. Shih, Q.G. Xu, G. Swaminathan, et al., A dense poly(ethylene glycol) coating improves penetration of large polymeric nanoparticles within brain tissue, Sci. Transl. Med. 4 (2012) 149 ra19.

[9] A.J. Sawyer, J.M. Piepmeier, W.M. Saltzman, New methods for direct delivery of chemotherapy for treating brain tumors, Yale J. Biol. Med. 79 (2006) 141–152.

[10] E. Allard, C. Passirani, J.P. Benoit, Convection-enhanced delivery of nanocarriers for the treatment of brain tumors, Biomaterials 30 (2009) 2302–2318.

[11] F. Lefranc, J. Brotchi, R. Kiss, Possible future issues in the treatment of glioblastomas: special emphasis on cell migration and the resistance of migrating glioblastoma cells to apoptosis, J. Clin. Oncol. 23 (2005) 2411–2422.

[12] L.G. Menon, V.J. Shi, R.S. Carroll, Mesenchymal Stromal Cells as a Drug Delivery System, 2008.

[13] A. Ebrahimi, N. Lalvand, Drug Delivery using genetically modified Mesenchymal Stem Cells: a promising targeted-delivery method. Hygeia, J. Drugs Med. 5 (2013) 90–104.

[14] M.R. Reagan, D.L. Kaplan, Concise review: mesenchymal stem cell tumor-homing: detection methods in disease model systems, Stem Cells 29 (2011) 920–927.

[15] J.K.Y. Chan, P.Y.P. Lam, Human mesenchymal stem cells and their paracrine factors for the treatment of brain tumors, Cancer Gene Ther. 20 (2013) 539–543.

[16] I.V. Balyasnikova, M.S. Prasol, S.D. Ferguson, Y. Han, A.U. Ahmed, M. Gutova, et al., Intranasal delivery of mesenchymal stem cells significantly extends survival of irradiated mice with experimental brain tumors, Mol. Ther. 22 (2014) 140–148.

[17] A. Aleynik, K.M. Gernavage, Y. Mourad, L.S. Sherman, K. Liu, Y.A. Gubenko, et al., Stem cell delivery of therapies for brain disorders, Clin. Transl. Med. 3 (2014), 2001–1326.

[18] S. Amano, S. Li, C. Gu, Y. Gao, S. Koizumi, S. Yamamoto, et al., Use of genetically engineered bone marrow-derived mesenchymal stem cells for glioma gene therapy, Int. J. Oncol. 35 (2009) 1265–1270.

[19] C. Altaner, V. Altanerova, M. Cihova, K. Ondicova, B. Rychly, L. Baciak, et al., Complete regression of glioblastoma by mesenchymal stem cells mediated prodrug gene therapy simulating clinical therapeutic scenario, Int. J. Cancer 134 (2014) 1458–1465.

[20] A. Nakamizo, F. Marini, T. Amano, A. Khan, M. Studeny, J. Gumin, et al., Human bone marrow-derived mesenchymal stem cells in the treatment of gliomas, Cancer Res. 65 (2005) 3307–3318.

[21] X.J. Tang, J.T. Lu, H.J. Tu, K.M. Huang, R. Fu, G. Cao, et al., TRAIL-engineered bone marrow-derived mesenchymal stem cells: TRAIL expression and cytotoxic effects on C6 glioma cells, Anticancer Res. 34 (2014) 729–734.

[22] S.M. Kim, J.S. Woo, C.H. Jeong, C.H. Ryu, J.D. Jang, S.S. Jeun, Potential application of temozolomide in mesenchymal stem cell-based TRAIL gene therapy against malignant glioma, Stem Cells Transl. Med. 3 (2014) 172–182.

[23] Q. Li, O. Wijesekera, S.J. Salas, J.Y. Wang, M. Zhu, C. Aprhys, et al., Mesenchymal stem cells from human fat engineered to secrete BMP4 are non-oncogenic, suppress brain cancer, and prolong survival, Clin. Cancer Res. 20 (2014) 2375–2387.

[24] S.G.M. Piccirillo, A.L. Vescovi, Bone morphogenetic proteins regulate tumorigenicity in human glioblastoma stem cells, Ernst. Scher. Found. 5 (2007) 59–81.

[25] Y. Feng, M. Zhu, S. Dangelmajer, Y.M. Lee, O. Wijesekera, C.X. Castellanos, et al., Hypoxia-cultured human adipose-derived mesenchymal stem cells are non-oncogenic and have enhanced viability, motility, and tropism to brain cancer, Cell Death Dis. 6 (2015) e1797.

[26] C.L. Smith, K.L. Chaichana, Y.M. Lee, B. Lin, K.M. Stanko, T. O'Donnell, et al., Pre-exposure of human adipose mesenchymal stem cells to soluble factors enhances their homing to brain cancer, Stem Cells Transl. Med. 4 (2015) 239–251.

[27] C. Pendleton, Q. Li, D.A. Chesler, K. Yuan, H. Guerrero-Cazares, A. Quinones-Hinojosa, Mesenchymal stem cells derived from adipose tissue vs bone marrow: in vitro comparison of their tropism towards gliomas, PloS one 8 (2013) e58198.

[28] T. Kim, E. Momin, J. Choi, K. Yuan, H. Zaidi, J. Kim, et al., Mesoporous silica-coated hollow manganese oxide nanoparticles as positive T1 contrast agents for labeling and MRI tracking of adipose-derived mesenchymal stem cells, J. Am. Chem. Soc. 133 (2011) 2955–2961.

[29] P.Y. Lam, X.O. Breakefield, Potential of gene therapy for brain tumors, Hum. Mol. Genet. 10 (2001) 777–787.

[30] R.A. Dewey, G. Morrissey, C.M. Cowsill, D. Stone, F. Bolognani, N.J. Dodd, et al., Chronic brain inflammation and persistent herpes simplex virus 1 thymidine kinase expression in survivors of syngeneic glioma treated by adenovirus-mediated gene therapy: implications for clinical trials, Nat. Med. 5 (1999) 1256–1263.

[31] S.A. Stohlman, D.R. Hinton, Viral induced demyelination, Brain Pathol. 11 (2001) 92–106.

[32] Q. Huang, J.P. Vonsattel, P.A. Schaffer, R.L. Martuza, X.O. Breakefield, M. DiFiglia, Introduction of a foreign gene (Escherichia coli lacZ) into rat neostriatal neurons using herpes simplex virus mutants: a light and electron microscopic study, Exp. Neurol. 115 (1992) 303–316.

[33] M.L. Albert, J.C. Darnell, A. Bender, L.M. Francisco, N. Bhardwaj, R.B. Darnell, Tumor-specific killer cells in paraneoplastic cerebellar degeneration, Nat. Med. 4 (1998) 1321–1324.

[34] N.G. Rainov, A phase III clinical evaluation of herpes simplex virus type 1 thymidine kinase and ganciclovir gene therapy as an adjuvant to surgical resection and radiation in adults with previously untreated glioblastoma multiforme, Hum. Gene Ther. 11 (2000) 2389–2401.

[35] G. Fulci, E.A. Chiocca, The status of gene therapy for brain tumors, Expert Opin. Biol. Ther. 7 (2007) 197–208.

[36] M. Thomas, A.M. Klibanov, Enhancing polyethylenimine's delivery of plasmid DNA into mammalian cells, P Natl. Acad. Sci. U. S. A. 99 (2002) 14640–14645.

[37] C.H. Ahn, S.Y. Chae, Y.H. Bae, S.W. Kim, Synthesis of biodegradable multi-block copolymers of poly(L-lysine) and poly(ethylene glycol) as a non-viral gene carrier, J. Control Release 97 (2004) 567–574.

[38] F.Q. Hu, M.D. Zhao, H. Yuan, J. You, Y.Z. Du, S. Zeng, A novel chitosan oligosaccharide-stearic acid micelles for gene delivery: properties and in vitro transfection studies, Int. J. Pharm. 315 (2006) 158–166.

[39] S. Spagnou, A.D. Miller, M. Keller, Lipidic carriers of siRNA: differences in the formulation, cellular uptake, and delivery with plasmid DNA, Biochem. Us 43 (2004) 13348–13356.

[40] D.G. Anderson, A. Akinc, N. Hossain, R. Langer, Structure/property studies of polymeric gene delivery using a library of poly(beta-amino esters), Mol. Ther. 11 (2005) 426–434.

[41] S.Y. Tzeng, J.J. Green, Subtle changes to polymer structure and degradation mechanism enable highly effective nanoparticles for siRNA and DNA delivery to human brain Cancer, Adv. Healthc. Mater. 2 (2013) 468–480.

[42] H. Guerrero-Cazares, S.Y. Tzeng, N.P. Young, A.O. Abutaleb, A. Quinones-Hinojosa, J.J. Green, Biodegradable polymeric nanoparticles show high efficacy and specificity at DNA delivery to human glioblastoma in vitro and in vivo, ACS Nano 8 (2014) 5141–5153.

[43] J. Sunshine, J.J. Green, K.P. Mahon, F. Yang, A.A. Eltoukhy, D.N. Nguyen, et al., Small-molecule end-groups of linear polymer determine cell-type gene-delivery efficacy, Adv. Mater. 21 (2009) 4947.

[44] A. Mangraviti, S.Y. Tzeng, K.L. Kozielski, Y. Wang, Y. Jin, D. Gullotti, et al., Polymeric nanoparticles for nonviral gene therapy extend brain tumor survival in vivo, ACS Nano 9 (2015) 1236–1249.

[45] M. Ying, Y. Sang, Y. Li, H. Guerrero-Cazares, A. Quinones-Hinojosa, A.L. Vescovi, et al., Kruppel-like family of transcription factor 9, a differentiation-associated transcription factor, suppresses Notch1 signaling and inhibits glioblastoma-initiating stem cells, Stem Cells 29 (2011) 20–31.

[46] N.S. Bhise, R.B. Shmueli, J. Gonzalez, J.J. Green, A novel assay for quantifying the number of plasmids encapsulated by polymer nanoparticles, Small 8 (2012) 367–373.

[47] S. Abbadi, J.J. Rodarte, A. Abutaleb, E. Lavell, C.L. Smith, W. Ruff, et al., Glucose-6-phosphatase is a key metabolic regulator of glioblastoma invasion, Mol. Cancer Res. MCR 12 (2014) 1547–1559.

[48] V. Kuch, C. Schreiber, W. Thiele, V. Umansky, J.P. Sleeman, Tumor-initiating properties of breast cancer and melanoma cells in vivo are not invariably reflected by spheroid formation in vitro, but can be increased by long-term culturing as adherent monolayers, Int. J. Cancer 132 (2013) E94–E105.

[49] T. Garzon-Muvdi, P. Schiapparelli, C. ap Rhys, H. Guerrero-Cazares, C. Smith, D.H. Kim, et al., Regulation of brain tumor dispersal by NKCC1 through a novel role in focal adhesion regulation, PLoS Biol. 10 (2012) e1001320.

[50] M. Zhu, Y. Feng, S. Dangelmajer, H. Guerrero-Cazares, K.L. Chaichana, C.L. Smith, et al., Human cerebrospinal fluid regulates proliferation and migration of stem cells through insulin-like growth factor-1, Stem Cells Dev. 24 (2015) 160–171.

[51] K.C. Kondapalli, J.P. Llongueras, V. Capilla-Gonzalez, H. Prasad, A. Hack, C. Smith, et al., A leak pathway for luminal protons in endosomes drives

oncogenic signalling in glioblastoma, Nat. Commun. 6 (2015) 6289.
[52] R. Grossman, H. Brastianos, J.O. Blakeley, A. Mangraviti, B. Lal, P. Zadnik, et al., Combination of anti-VEGF therapy and temozolomide in two experimental human glioma models, J. Neuro Oncol. 116 (2014) 59–65.
[53] D. Li, M. Zhang, Q. Zhang, Y. Wang, X. Song, Q. Zhang, Functional recovery after acute intravenous administration of human umbilical cord mesenchymal stem cells in rats with cerebral ischemia-reperfusion injury, Intractable Rare Dis. Res. 4 (2015) 98–104.
[54] H. Yin, R.L. Kanasty, A.A. Eltoukhy, A.J. Vegas, J.R. Dorkin, D.G. Anderson, Non-viral vectors for gene-based therapy, Nat. Rev. Genet. 15 (2014) 541–555.
[55] C. Baum, O. Kustikova, U. Modlich, Z.X. Li, B. Fehse, Mutagenesis and oncogenesis by chromosomal insertion of gene transfer vectors, Hum. Gene Ther. 17 (2006) 253–263.
[56] N. Bessis, F.J. GarciaCozar, M.C. Boissier, Immune responses to gene therapy vectors: influence on vector function and effector mechanisms, Gene Ther. 11 (2004). S10–S7.
[57] A. Nauta, C. Seidel, L. Deveza, D. Montoro, M. Grova, S.H. Ko, et al., Adipose-derived stromal cells overexpressing vascular endothelial growth factor accelerate mouse excisional wound healing, Mol. Ther. 21 (2013) 445–455.
[58] D. Fischer, T. Bieber, Y.X. Li, H.P. Elsasser, T. Kissel, A novel non-viral vector for DNA delivery based on low molecular weight, branched polyethylenimine: effect of molecular weight on transfection efficiency and cytotoxicity, Pharm. Res. 16 (1999) 1273–1279.
[59] M.A. Gosselin, W.J. Guo, R.J. Lee, Efficient gene transfer using reversibly cross-linked low molecular weight polyethylenimine, Bioconjug. Chem. 12 (2001) 989–994.
[60] S.G. Piccirillo, B.A. Reynolds, N. Zanetti, G. Lamorte, E. Binda, G. Broggi, et al., Bone morphogenetic proteins inhibit the tumorigenic potential of human brain tumour-initiating cells, Nature 444 (2006) 761–765.
[61] K.L. Chaichana, L. Kone, C. Bettegowda, J.D. Weingart, A. Olivi, M. Lim, et al., Risk of surgical site infection in 401 consecutive patients with glioblastoma with and without carmustine wafer implantation, Neurol. Res. 37 (2015) 717–726.
[62] R. Grossman, P. Burger, E. Soudry, B. Tyler, K.L. Chaichana, J. Weingart, et al., MGMT inactivation and clinical response in newly diagnosed GBM patients treated with Gliadel, J. Clin. Neurosci. Off. J. Neurosurg. Soc. Australas. 22 (2015) 1938–1942.
[63] M.J. McGirt, K.D. Than, J.D. Weingart, K.L. Chaichana, F.J. Attenello, A. Olivi, et al., Gliadel (BCNU) wafer plus concomitant temozolomide therapy after primary resection of glioblastoma multiforme, J. Neurosurg. 110 (2009) 583–588.
[64] F.J. Attenello, D. Mukherjee, G. Datoo, M.J. McGirt, E. Bohan, J.D. Weingart, et al., Use of Gliadel (BCNU) wafer in the surgical treatment of malignant glioma: a 10-year institutional experience, Ann. Surg. Oncol. 15 (2008) 2887–2893.
[65] A. Nakamizo, F. Marini, T. Amano, A. Khan, M. Studeny, J. Gumin, et al., Human bone marrow-derived mesenchymal stem cells in the treatment of gliomas, Cancer Res. 65 (2005) 3307–3318.
[66] J.M. Gimble, A.J. Katz, B.A. Bunnell, Adipose-derived stem cells for regenerative medicine, Circ. Res. 100 (2007) 1249–1260.
[67] N. Puissant, C. Barreau, P. Bourin, C. Clavel, J. Corre, C. Bousquet, et al., Immunomodulatory effect of human adipose tissue-derived adult stem cells: comparison with bone marrow mesenchymal stem cells, Brit J. Haematol. 129 (2005) 118–129.